ELSEVIER

Journal of Alloys and Compounds 227 (1995) 69–75

Journal of ALLOYS AND COMPOUNDS

Hydrogen absorption–desorption characteristics of $Ti_{0.35}Zr_{0.65}Ni_xV_{2-x-y}Mn_y$ alloys with C14 Laves phase for nickel/metal hydride batteries

H.W. Yang, S.N. Jenq, Y.Y. Wang *, C.C. Wan

Department of Chemical Engineering, National Tsing-Hua University, Hsinchu 30043, Taiwan

Received 9 December 1994; in final form 20 February 1995

Abstract

The properties of $Ti_{0.35}Zr_{0.65}Ni_xV_{2-x-y}Mn_y$ ($1.0 \le x \le 1.2$, $0.2 \le y \le 0.4$) alloys including crystallographic parameters, the enthalpy for hydride formation, pressure–composition–temperature (*P–C–T*) curves and electrochemical discharge capacities were investigated. Based on scanning electron microscopy results, with the exception of alloy A ($x = 1.0$, $y = 0.2$) which forms two distinguishable phases, alloys B ($x = 1.0$, $y = 0.4$), C ($x = 1.2$, $y = 0.2$) and D ($x = 1.2$, $y = 0.4$) all form single uniform phase. Structure contraction took place owing to partial replacement by nickel and/or manganese, but alloys B to D all exhibited C14 type Laves phases. The content of absorbed hydrogen increased as the d-electron concentration (DEC) of the alloys diminished. Although alloy A has the largest hydrogen absorption ability compared with the other alloys, this is not the case with respect to the hydrogen desorption ability of alloys. This can be attributed to the poor reversibility of hydriding–dehydriding of alloy A. It was found that the discharge capacities of alloys were affected not only by the content of absorbed hydrogen but also by the resistance to hydrogen release. Alloy C, $Ti_{0.35}Zr_{0.65}Ni_{1.2}V_{0.6}Mn_{0.2}$, possessing good hydriding–dehydriding properties in gas and liquid media, is a promising electrode material.

Keywords: Hydrogen absorption; Hydrogen desorption; Electrochemical discharge capacity

1. Introduction

Recently, the development of high-performance hydrogen absorbing alloys for nickel/metal hydride batteries has become active worldwide, because these batteries are fast replacing Ni/Cd batteries in consumer applications owing to energy and environmental concerns. Nickel/metal hydride batteries are also being intensively studied for electronic vehicle applications [1]. Previously, in our laboratory the pressure–composition–temperature (*P–C–T*) behavior of four-element alloys $Ti_xZr_{1-x}Ni_yV_{2-y}$ ($x = 0.0$, 0.5, 1.0; $y = 0.0$, 1.0, 2.0) were studied and the response surface function of hydrogen desorption of these alloys was calculated by Yates' algorithm [2]. However, all the systems exhibited irreversible hydriding–dehydriding properties and had rather sloped *P–C–T* curves. According to a scanning electron microscopy (SEM) investigation, all the alloys were multiphase. Jordy et al. [3] found that the AB_2 type alloy $Ti_{0.17}Zr_{0.16}Ni_{0.34}V_{0.33}$ is multiphase polycrystalline and also has a sloped *P–C–T* curve. Obviously, hydrides formed by alloys with certain phases are so stable that they cannot release the absorbed hydrogen easily. Because the reversibility of hydriding–dehydriding of these alloys is poor, they are not suitable for electrode material. In our laboratory the substitutional effect of Ni and Mn for V in the alloy $Ti_{0.35}Zr_{0.65}Ni_{0.6}V_{1.4}$ was also studied, and the result shows that the Mn containing alloy has a more uniform structure, thus improving the hydrogen desorption ability. Similarly, Miyamura et al. [4] have demonstrated that the replacement of the site B element by Mn in AB_2 alloys can improve the electrochemical discharge capacity of the alloy. Accordingly, five-element alloys such as Ti–Zr–Ni–V–Mn seem to have good hydrogen absorbing properties. In this study the alloy $Ti_{0.35}Zr_{0.65}Ni_xV_{2-x-y}Mn_y$ ($1.0 \le x \le 1.2$, $0.2 \le y \le 0.4$) was investigated regarding its crystallographic parameters, thermodynamic properties, pressure–composition isotherm and electrochemical discharge capacity. Hopefully, more information pertaining to its potentially superior performance and a possible explanation related to its structure can be obtained from this research.

* Corresponding author.

SSDI 0925-8388(95)01607-4

2. Experimental

Hydrogen-absorbing alloys were prepared using an arc-melting furnace under argon atmosphere. The purity of the metals was at least 99.5 wt.%. To assure the homogeneity of the alloy, the ingot was turned over and remelted at least 14 times.

The ingots were then pulverized first by hydriding–dehydriding and finally by ball-milling. Powder with particle size less than 230 mesh was used in *P–C–T* measurements and powder of size less than 325 mesh was used as electrode material.

The *P–C–T* characteristics were measured by a high-pressure volumetric system [5]. About 5 g sample powder was taken for each test run. For activation, alloy powder was first evacuated and then exposed to hydrogen atmosphere at a pressure of 5 kg cm^{-2} as heated to 350 °C for 1.5 h at the same time. Dehydriding was performed by evacuating and heating the hydrided powder at 350 °C for 2.5 h. After two cycles of activation, desorption *P–C–T* data were recorded.

Alloy pieces with different compositions were polished for study of the microstructure. The morphology was observed by SEM (JSM-840A scanning microscope). Lattice structures of the alloy were investigated by X-ray diffraction (XRD) with Cu Kα radiation.

The metal hydride electrodes were made by mixing alloy powder (less than 325 mesh) with nickel powder (less than 3 μm) at a weight ratio of 1:3. 3 wt.% polytetrafluoroethylene (PTFE) dispersion was added to the mixture as binder. The mixture was cold pressed onto an Ni mesh under a pressure of 1 ton cm^{-2}. The apparent surface area of the electrode was 2.5×2.5 cm^2 and the thickness of the electrode was about 1.6 mm.

The electrochemical cell consisted of the working electrode (metal hydride alloy powder electrode), counter electrode ($NiOOH/Ni(OH)_2$ electrode), and reference electrode (Hg/HgO electrode). The working electrode was enclosed with a non-woven nylon separator (Pellon 2516) and then inserted between two counter electrodes. They were held tightly together in a Teflon holder and 30 wt.% KOH solution was used as electrolyte. The discharge capacity of each sample was determined by a galvanostatic method. The cut-off voltage for discharging was fixed at -700 mV with respect to the Hg/HgO electrode. Readings were taken after several charging–discharging cycles to ensure that the hydride electrode was activated completely.

3. Results and discussion

3.1. Physical properties and hydrogen absorption–desorption behavior of alloys

Jordy et al. [3] investigated the hydriding–dehydriding properties of AB_2 type hydrogen absorbing alloy with nominal composition $Ti_{0.17}Zr_{0.16}Ni_{0.34}V_{0.33}$. They found that this alloy has a multiphase polycrystalline structure and has a sloped *P–C–T* curve. Since the hydrogen content is still about 0.8 H mol^{-1} at a hydrogen pressure below 0.01 bar, they attributed this to the formation of a very stable hydride. Similarly, we also found that the four-element alloy $Ti_{0.35}Zr_{0.65}Ni_{0.6}V_{1.4}$ which forms three main phases has the maximum hydrogen desorption ability among the alloys $Ti_xZr_{1-x}Ni_yV_{2-y}$ ($0.0 \le x \le 1.0$, $0.0 \le y \le 2.0$), but from *P–C–T* data there was still 1.43 wt.% hydrogen trapped in the alloy bulk at a hydrogen pressure less than 0.01 atm. Accordingly, there must be some phases within the alloy which form stable hydrides that are irreversible under hydriding–dehydriding. In the meantime, we also found that partial replacement of V by Mn and Ni in alloy $Ti_{0.35}Zr_{0.65}Ni_{0.6}V_{1.4}$ can improve the phase uniformity, hence improving the reversibility of hydriding–dehydriding. Miyamura et al. [4] also stated that replacement of the site B element by Mn in AB_2 type hydrogen absorbing alloy can enhance the electrochemical discharge capacity of the alloy. It is obvious that partial replacement of the site B element by Mn and/or Ni enhances the reversibility of hydriding–dehydriding of the alloy. Therefore, the properties of alloys with Ti–Zr–Ni–V–Mn as host elements are worth further study. Since the alloy $Ti_{0.35}Zr_{0.65}Ni_{0.6}V_{1.4}$ has been well studied, the substitutional effects of Mn and/or Ni for V of this alloy were investigated. The nominal composition of the alloy being studied can be expressed as $Ti_{0.35}Zr_{0.65}Ni_xV_{2-x-y}Mn_y$ ($1.0 \le x \le 1.2$, $0.2 \le y \le 0.4$). To make the experiments more efficient, an experimental design method was used. Here a 2^2 factorial design [6] was adopted and four compositions were prepared. Let $x = 1.0$ or 1.2 and $y = 0.2$ or 0.4, the compositions of alloys are then $Ti_{0.35}Zr_{0.65}Ni_{1.0}V_{0.8}Mn_{0.2}$ (alloy A), $Ti_{0.35}Zr_{0.65}Ni_{1.0}V_{0.6}Mn_{0.4}$ (alloy B), $Ti_{0.35}Zr_{0.65}Ni_{1.2}V_{0.6}Mn_{0.2}$ (alloy C) and $Ti_{0.35}Zr_{0.65}Ni_{1.2}V_{0.4}Mn_{0.4}$ (alloy D) respectively.

Scanning electron micrographs of alloys A to D are shown in Fig. 1. It is clear that except for alloy A, the alloys are nearly a uniform phase. This implies that alloys B to D may have better reversibility of hydriding–dehydriding than alloy A. Fig. 2 shows the equilibrium hydrogen pressure with respect to hydrogen concentration absorbed in the alloy. Below 0.01 atm, there is 0.93 wt.% hydrogen atoms stored in alloy A which is considerably more than the amounts of alloys B to D. For easy comparision, we define the reversibility of hydriding–dehydriding of the alloy as follows:

$$R(\%) = \frac{\text{the content of hydrogen in the alloy (between 0.01 and 10 atm)}}{\text{the content of hydrogen in the alloy (at 10 atm)}} \times 100$$

The reversibility of hydriding–dehydriding of alloys A to D can then be computed as follows:

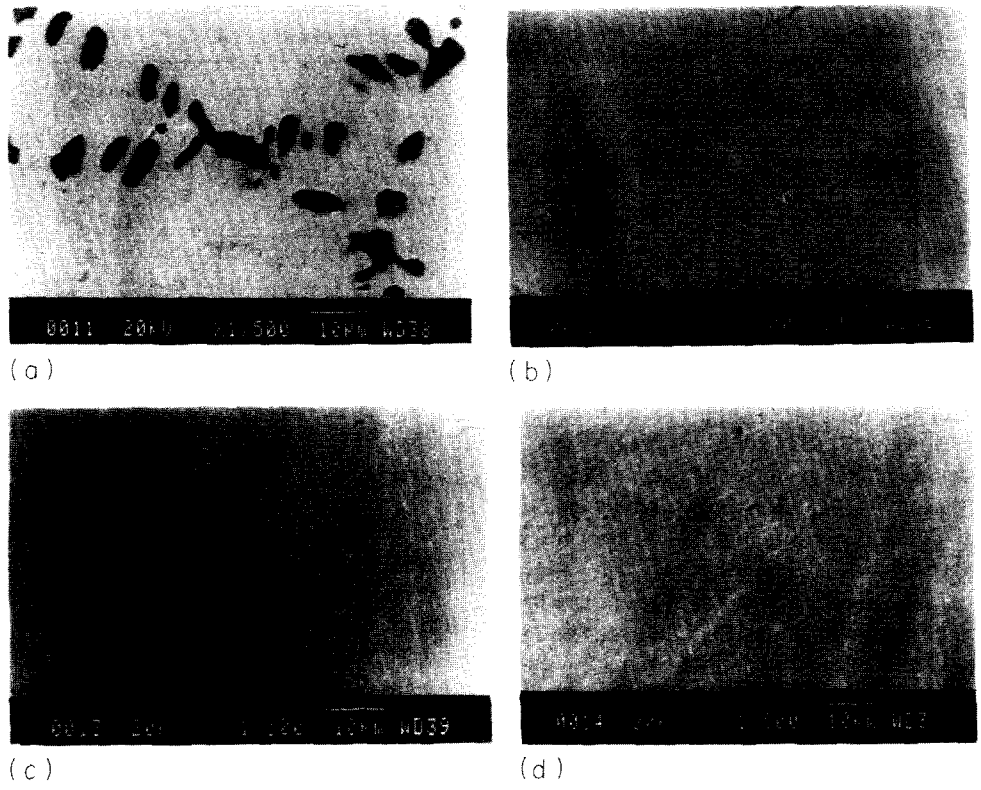

Fig. 1. Scanning electron micrographs of (a) alloy A, (b) alloy B, (c) alloy C and (d) alloy D.

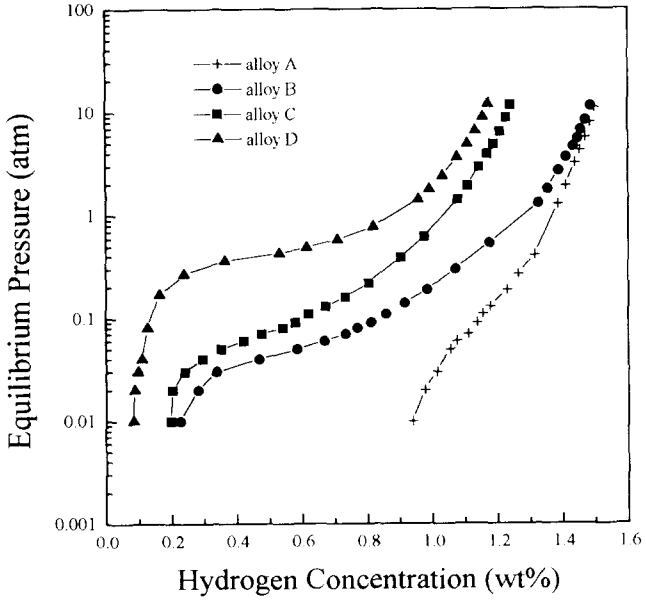

Fig. 2. Equilibrium hydrogen pressure vs. hydrogen concentration (weight per cent) at 40 °C for alloys A to D.

$$R_A(\%) = \frac{1.50-0.93}{1.50} \times 100 = 38$$

$$R_B(\%) = \frac{1.48-0.23}{1.48} \times 100 = 84$$

$$R_C(\%) = \frac{1.23-0.20}{1.23} \times 100 = 84$$

$$R_D(\%) = \frac{1.17-0.08}{1.17} \times 100 = 93$$

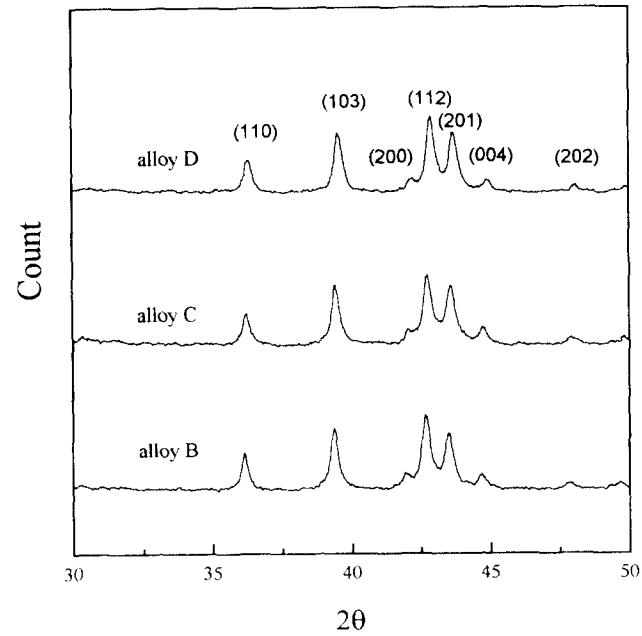

Fig. 3. X-ray diffraction patterns of alloys B to D.

Table 1
Crystallographic parameters for selected $Ti_{0.35}Zr_{0.65}Ni_xV_{2-x-y}Mn_y$ ($1.0 \le x \le 1.2$, $0.2 \le y \le 0.4$) alloys

Compound (nominal compositions)	Alloy identification	Lattice constant a/c (Å)	Unit cell volume (Å^3)	Crystal structure
$Ti_{0.35}Zr_{0.65}Ni_{1.0}V_{0.8}Mn_{0.2}$	A	N.A.	N.A.	N.A.
$Ti_{0.35}Zr_{0.65}Ni_{1.0}V_{0.6}Mn_{0.4}$	B	4.97/8.11	173.17	C14
$Ti_{0.35}Zr_{0.65}Ni_{1.2}V_{0.6}Mn_{0.2}$	C	4.95/8.10	171.91	C14
$Ti_{0.35}Zr_{0.65}Ni_{1.2}V_{0.4}Mn_{0.4}$	D	4.94/8.07	170.76	C14

The reversibility of alloy A (R_A) is substantially lower than that of the other alloys. Since alloy A is multiphase, this may be because one of the phases of alloy A forms a stable hydride.

The XRD results of alloys B to D are illustrated in Fig. 3. It can be seen that the XRD patterns of alloys B to D are consistent with the $Ti_{0.8}Zr_{0.2}Mn_{0.8}Cr_{1.2}$ Laves phase alloy and has C14 type lattice structure [7]. This shows that if the content of V is less than 0.8 in alloy $Ti_{0.35}Zr_{0.65}Ni_xV_{1-x-y}Mn_y$, the C14 type Laves phase can be formed. The lattice constants of alloys B to D are listed in Table 1. The c/a ratios are about 1.63, which are within the range 1.63–1.65 as reported in the literature for AB_2 alloys with C14 type structure [7]. The cell volumes of the sample alloys are between 170.76 and 173.17 Å^3 and they decrease as the contents of Ni and Mn in the alloy increase. This is in good agreement with the size-order of the atoms (V > Mn > Ni) if we assume Mn and Ni occupy the V sites. A similar phenomenon was also reported by Bernauer and Halene [8].

Laves phases belong to an important group of size factor intermetallic compounds. In addition to the geometric factors, the electronic effects should also be taken into account to demonstrate the stability of Laves phases. According to Elliot and Rostocker [9], there is a correlation between the average number of outer electrons (ANOE) and the occurrence of C14 and C15 structures for TiB_2 and ZrB_2 compounds (where B is V, Cr, Mn, Fe, Cu, and Zn). When the ANOE of an alloy is between 5.4 and 7.0, both Ti and Zr systems form C14 type Laves phase structure, because if the value of ANOE of the alloy is between 5.4 and 7.0, a stable C14 structure alloy can be formed. For alloys B to D, the ANOE values are calculated as follows:

$$ANOE_B = \frac{(0.35)(4) + (0.65)(4) + (1.0)(10) + (0.6)(5) + (0.4)(7)}{3} = 6.60$$

$$ANOE_C = \frac{(0.35)(4) + (0.65)(4) + (1.2)(10) + (0.6)(5) + (0.2)(7)}{3} = 6.80$$

$$ANOE_D = \frac{(0.35)(4) + (0.65)(4) + (1.2)(10) + (0.4)(5) + (0.4)(7)}{3} = 6.93$$

The ANOE values for alloys B to D are within the range 5.4–7.0, and these alloys do form the C14 structure. This means that the finding of Elliot and Rostocker can be used to judge whether $Ti_{0.35}Zr_{0.65}Ni_xV_{2-x-y}Mn_y$ ($1.0 \le x \le 1.2$, $0.2 \le y \le 0.4$) systems form C14 type alloy and may perform as a pseudo binary alloy.

Fig. 2 further shows that alloy A contains the largest amount of absorbed hydrogen, followed by alloy B, alloy C and finally alloy D. From Table 1, although lattice contraction occurs from alloy B to alloy D, all the alloys are pure C14 type Laves phase structures and the hydrogen absorption capacity of the alloys decreases as the unit cell volume of the alloys is decreased. The d-electron concentrations (DEC) of alloys B to D are calculated as follows:

$$DEC_B = \frac{(0.35)(2) + (0.65)(2) + (1)(8) + (0.6)(3) + (0.4)(5)}{3} = 4.60$$

$$DEC_C = \frac{(0.35)(2) + (0.65)(2) + (1.2)(8) + (0.6)(3) + (0.2)(5)}{3} = 4.80$$

$$DEC_D = \frac{(0.35)(2) + (0.65)(2) + (1.2)(8) + (0.4)(3) + (0.4)(5)}{3} = 4.93$$

Based on the concept of the DEC of alloys, it seems that the content of absorbed hydrogen of alloys B, C, and D increases as the DEC of the alloy is decreased. Studies of hydriding characteristics of alloys based on the TiFe, TiCrMn and TiVMn systems have demonstrated that the degree of

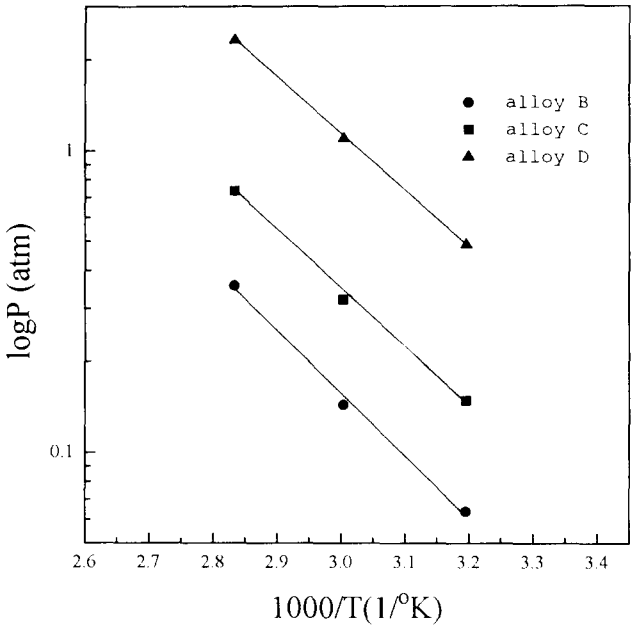

Fig. 4. The van't Hoff plot for alloy–hydrogen systems.

hydrogen absorption depends on the concentration of valence electrons and especially on the d-electron concentration (DEC) [10]. Bernauer et al. [11] studied the absorption of hydrogen by C14 and C15 type Laves phase alloys and they concluded that the alloys of 3d transition metals store hydrogen in the metal lattice until the 3d orbital is half full. Summarizing the results above, we can propose that the hydrogen absorption capacity of alloys with C14 and/or C15 Laves phase increases as the DEC of the alloys is decreased. Consequently, the DEC of the alloy can be a good indicator to predict the hydrogen absorption capacity.

Qualitatively, the higher the plateau pressure is, the smaller the enthalpy of hydride formation. From Fig. 2 the equilibrium plateau pressures are ca. 0.04, 0.07, 0.40 atm for alloys B, C and D respectively. Accordingly, the absolute value of enthalpy of hydride formation should be in the order alloy B > alloy C > alloy D. The enthalpy of hydride formation can be calculated by the following equation [12]:

$$\Delta G = \Delta H - T\Delta S = RT \ln P \quad (1)$$

where ΔG is the change in Gibbs free energy of hydride formation, P is the equilibrium hydrogen pressure, ΔH is the enthalpy for hydride formation, ΔS is the entropy change for hydride formation, and R is the gas constant.

Plotting ln P vs. $(1/T)$ should produce a straight line with the slope and intercept being $\Delta H/R$ and $\Delta S/R$. Hence ΔH and ΔS can be obtained. Fig. 4 is the van't Hoff plot for alloys B to D. The values of ΔH for alloys B to D are -9.43, -8.76 and -8.64 kcal mol H_2^{-1} respectively and they are consistent with the tendency predicted by the plateau pressures from P–C–T curves. These data are within the same range as the value for $Ti_{0.8}Zr_{0.2}Cr_{0.8}Mn_{1.2}$ which is -6.9 kcal mol H_2^{-1} [13]. Ovshinsky et al. [12] stated that if the ΔH value is between -6 and -12 kcal mol H_2^{-1}, the alloy is suitable for battery application. Thus alloys B to D are potential candidates for electrode material.

3.2. Electrochemical characteristics of alloys

In the previous section, the dependence of the reversibility of hydriding–dehydriding on the phase distribution of the alloy was discussed. That the hydriding–dehydriding performance in gas phase of alloys B to D is superior to that of alloy A is due to the possible formation of a stable hydride in alloy A. Because hydriding–dehydriding of alloys occurs similarly in gas and liquid media, it is likely that the electrochemical performance of alloys B to D is better than that of alloy A.

Fig. 5 shows the discharge capacities of alloys A to D at various discharge current densities at 30 °C. Figs. 6 and 7 illustrate the discharge characteristics of electrodes prepared from different alloys at different current densities. The results in Figs. 5–7 in general indicate that the discharge performances of alloys B to D are superior to that of alloy A. A closer look at Fig. 5 shows that at low discharge current densities (less than 150 mA g^{-1}), the discharge capacities of the alloys are in the order alloy C > alloy B > alloy D. However, this is not consistent with the contents of hydrogen absorbed in the alloys, which are ranked alloy B > alloy C > alloy D. Recalling that the enthalpy of hydride formation of alloy B (-9.43 kcal mol H_2^{-1}) is more negative than those of alloy C (-8.76 kcal mol H_2^{-1}) and alloy D (-8.64 kcal mol H_2^{-1}), which may induce a larger resistance regarding hydrogen release during discharge, we think that the smaller discharge capacity of alloy B than that of alloy C is reasonable. This means that the electrochemical discharge capacities

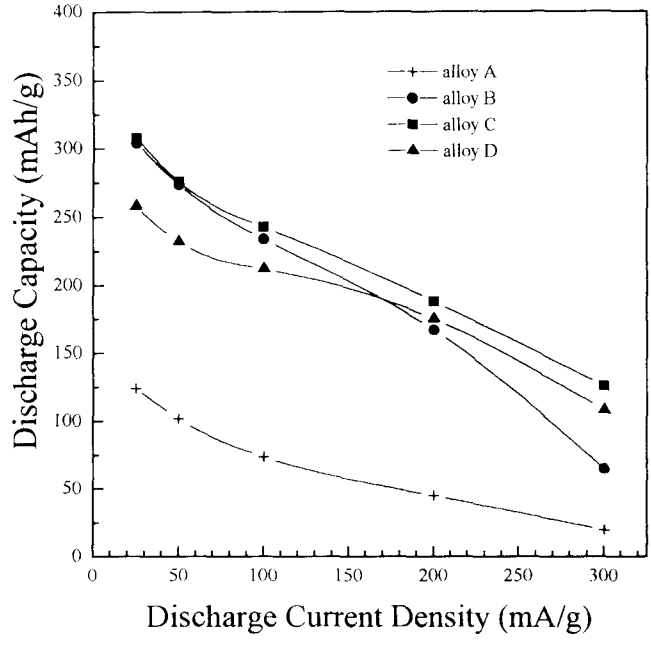

Fig. 5. The discharge capacities of alloys in response to current densities at 30 °C.

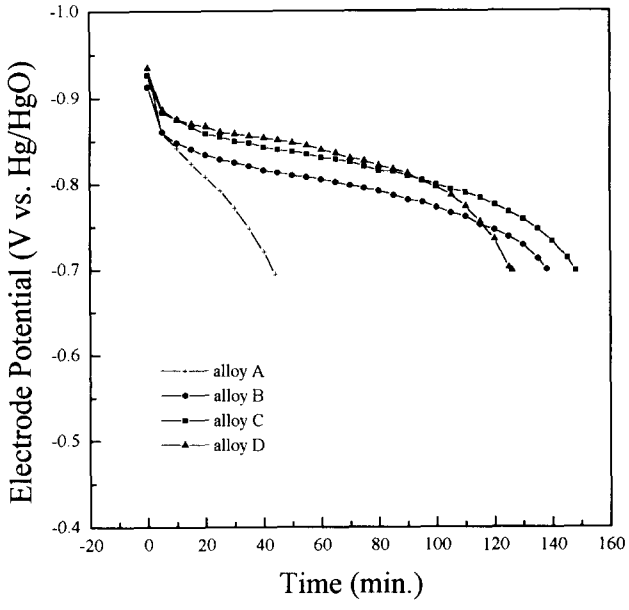

Fig. 6. Discharge behavior of electrodes prepared with different alloys at 100 mA g^{-1} discharge current density and 30 °C.

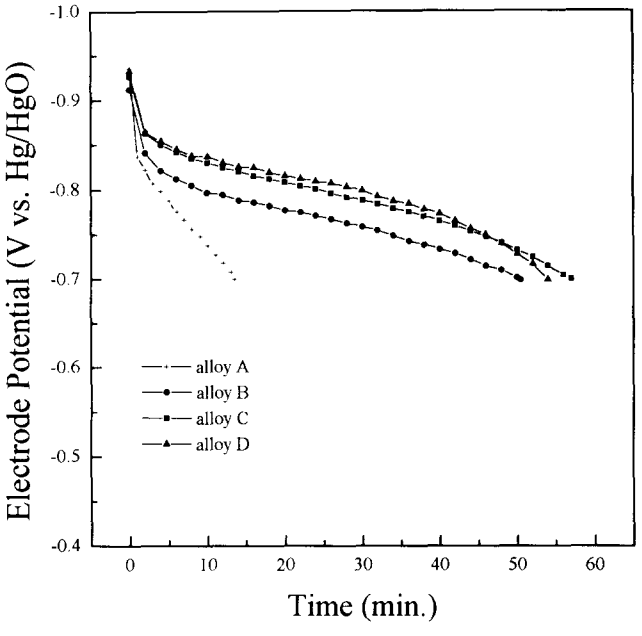

Fig. 7. Discharge behavior of electrodes prepared with different alloys at 200 mA g^{-1} discharge current density and 30 °C.

of alloys are determined not only by the content of absorbed hydrogen of the alloy but also by the enthalpy value of hydride formation. However, Fig. 5 shows that under high rate discharge (greater than 150 mA g^{-1}), the decrease in discharge capacity of alloy B is more pronounced than those of alloy C and alloy D as the discharge current density is increased, which means that at high discharge rate the resistance to hydrogen release becomes the controlling factor. As a result, alloy C has maximum discharge capacity followed by alloy D and finally alloy B.

Another interesting point concerns the closed-circuit voltage (CCV) of the electrode. A closer look at Fig. 6 or Fig. 7 shows that in the major range of discharge time alloy D has the highest CCV followed by alloy C and alloy B. Hence, voltage regulation of batteries can be obtained by proper adjustment of the alloying elements.

Statistical analysis of the capacities of various alloys is shown in Fig. 8. The nominal composition of the alloys is $Ti_{0.35}Zr_{0.65}Ni_xV_{2-x-y}Mn_y$, where x is the change in Ni content, y is the change in Mn content. If 1 represents the low level of factors x and y and 2 represents the high level of factors x and y, then x_1 and x_2 represent factor x at low and high levels respectively. Similarly, y_1 and y_2 represent factor y at low and high levels. Consequently, x_1y_1, x_1y_2, x_2y_1 and x_2y_2 represent alloy A, alloy B, alloy C and alloy D respectively. According to Montgomery [6], the effect (which is defined to be the change in response produced by a change in the level of the factor) of x is

$$p = \frac{1}{2}[210 + 247 - 230 - 73] = 77$$

and the effect of y is

$$q = \frac{1}{2}[210 + 230 - 247 - 73] = 60$$

and the interaction between factors x and y is

$$pq = \frac{1}{2}[210 + 73 - 247 - 230] = -97$$

Since $pq(-97)$ is substantially higher than $p(77)$ and $q(60)$ and, in Fig. 8, lines y_1 and y_2 cross, there is significant inter-

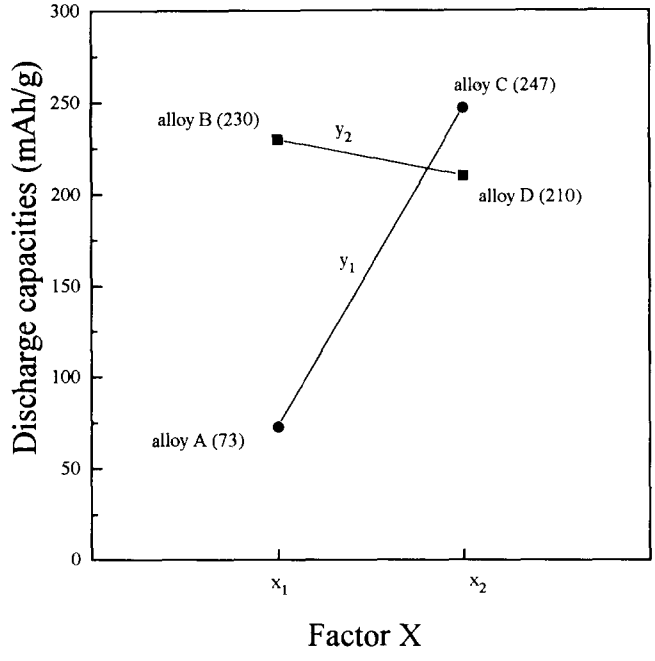

Fig. 8. Response data of discharge capacities for alloys A to D at 100 mA g^{-1} discharge current density with 2^2 factorial experiment design.

action between factors x and y. Therefore, the effect of x depends on the level chosen for factor y (i.e. if we change the Ni content, the corresponding change in discharge capacity is different according to the Mn content in the alloy and vice versa). The response of capacities under different discharge conditions also shows strong interaction between factors x and y.

4. Conclusion

The properties and structure of $Ti_{0.35}Zr_{0.65}Ni_xV_{2-x-y}Mn_y$ ($1.0 \leq x \leq 1.2$, $0.2 \leq y \leq 0.4$) alloys were investigated. Some significant results are summarized as follows.

(1) The unit cell volume of the alloys is changed by the replacement of V by Ni and/or Mn. The alloys form a uniform phase with C14 type Laves structure when the content of V is less than 0.8.

(2) The hydrogen absorption ability of alloys with C14 type Laves phase increases as the d-electron concentration (DEC) of the alloys is decreased. However, the capacity of hydrogen absorption is not the only factor controlling the amount of hydrogen release during discharge. The resistance to hydrogen release is another factor which becomes especially important at high discharge rate.

(3) Alloy C, $Ti_{0.35}Zr_{0.65}Ni_{1.2}V_{0.6}Mn_{0.2}$, was found to be a potential material for battery application.

Acknowledgements

The authors would like to express their thanks for financial support by the National Science Council of the Republic of China under project No. NSC-82-0402-E007-250 and by Pao-Chang Company.

References

[1] A. Anani, A. Visintin, K. Petrov and S. Srinivasan, *J. Power Sources, 47* (1994) 261–275.
[2] G.E.P. Box and N.R. Draper (eds.), *Empirical Model-Building and Response Surfaces*, Wiley, New York, 1987.
[3] C. Jordy, J. Bouet, P. Sanchez, C. Chanson and J. Leonardi, *J. Less-Common Met., 172–174* (1991) 1236.
[4] H. Miyamura, T. Sakai, N. Kuriyama, K. Oguro, A. Kato and H. Ishikawa, in D.A. Corrigan and S. Srinivasan (eds.), *Proc. Symp. on Hydrogen Storage Materials, Batteries and Electrochemistry*, Electrochemical Society, Pennington, NJ, p. 179.
[5] J.J. Reily and R.H. Wiswall, *J. Inorg. Chem., 6* (1967) 2220.
[6] D.C. Montgomery, *Design and Analysis of Experiments*, 1984, 2nd edn.
[7] Y. Moriwaki, T. Gamo and T. Iwaki, *J. Less-Common Met., 172–174* (1991) 1028.
[8] O. Bernauer and C. Halene, *J. Less-Common Met., 131* (1987) 213.
[9] R.P. Elliot and W. Rostocker, *Trans. Am. Soc. Met., 50* (1958) 617.
[10] J.J. Reilly, in A.F. Andresen and A.J. Maeland (eds.), *Int. Symp. on Hydride for Energy Storage*, William Clowes, 1977, p. 301.
[11] O. Bernauer, J. Topler, D. Noreus, R. Hempelmann and D. Richter, *Int. J. Hydrogen Energy, 14* (1989) 187.
[12] S.R. Ovshinsky, M.A. Fetcenko and J. Ross, *Science, 260* (1993) 176.
[13] Y. Machida, T. Yamadaya and M. Asanuma, in A.F. Andresen and A.J. Maeland (eds.), *Int. Symp. on Hydride for Energy Storage*, William Clowes, 1977, p. 329.